

Investigation of Crosslinking in the Thermooxidative Aging of Nitrile–Butadiene Rubber

Jiaohong Zhao,¹ Rui Yang,¹ Rossana Iervolino,² Stellario Barbera²

¹Key Laboratory of Advanced Materials (Ministry of Education), Department of Chemical Engineering, Tsinghua University, Beijing 100084, People's Republic of China

²Engineering and Research Center, SKF B.V., Kelvinbaan 16, 3439 MT Nieuwegein, the Netherlands

Correspondence to: R. Yang (E-mail: yangr@mail.tsinghua.edu.cn)

ABSTRACT: Chemical crosslinking is possibly the most significant factor affecting the mechanical behavior of rubbers. In this study, we investigated the evolution of network structures (the crosslinking degree and crosslinking density) during the thermooxidative aging of a nitrile–butadiene rubber (NBR) using characterization methods such as low-dimensional NMR, solvent extraction, solvent swelling, IR spectroscopy, and mechanical property measurements. The NMR and solvent extraction results show the change of the crosslinking degree. The solvent swelling results show the change of the crosslinking density. The IR results show the chemical changes relating to crosslinking and chain scissions. Therefore, a comprehensive picture of the thermal oxidative aging of the NBR compound was drawn by the integration of various results from these methods. Crosslinking occurred throughout the aging process, whereas chain scissions took place and competed with crosslinking in the later stage. The crosslinking density increased at a nearly constant rate, whereas the increase in the crosslinking degree slowed down in the later stage. The crosslinking density was closely correlated with the hardness and Young's modulus. © 2014 Wiley Periodicals, Inc. *J. Appl. Polym. Sci.* **2015**, *132*, 41319.

KEYWORDS: aging; crosslinking; rubber

Received 23 March 2014; accepted 20 July 2014

DOI: 10.1002/app.41319

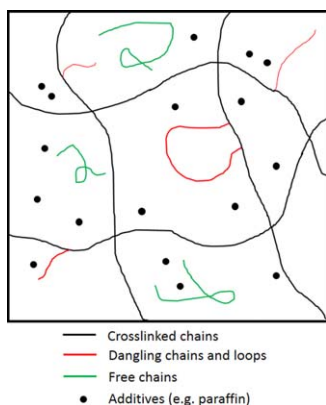
INTRODUCTION

During the thermooxidative aging of rubbers, changes in the network structure (the crosslinking degree or crosslinking density) often happen; this results in changes in the mechanical properties, including the tensile strength, tensile modulus, elongation at break, tear strength, compression set, and stress at certain strains.^{1–3} Some unvulcanized sulfurs in ethylene-propylene-diene rubber (EPDM) can continue to vulcanize during the thermoaging process.⁴ At high temperatures, unstable crosslinks can be broken down. For example, a peroxide-cured styrene–butadiene rubber/poly(ethylene-co-vinyl acetate) blend continuously crosslinked when aged at 70°C, with a slight increase in its tensile strength.⁵ On the other hand, an increase in the temperature could destroy the crosslink network and, in turn, the tensile properties. The covalent crosslinking density of a natural rubber/zinc dimethacrylate composite decreased after thermal aging at 80 and 100°C, whereas the ionic crosslinking density was stable at a relatively low temperature (80°C).¹ Instead, in the case of chloroprene rubber, crosslink formation was dominant during the aging process. The modulus increased, and both the tensile strength and the ultimate elongation decreased because of the decrease in the flexibility of the

structural network.⁶ For nitrile–butadiene rubber (NBR), the crosslinking reaction happened with increasing rigidity during thermal oxidative aging at 100°C.⁷ New unsaturated sites generated at 140°C could have been the nuclei of crosslinking.⁸ The mechanical properties and the chemical structural changes of NBR could be well correlated after aging for a long time.⁹

Various experimental methods to measure the crosslinking structure of polymers are available. Each of them is based on different physical principles and, therefore, provides a different perspective in elucidating the molecular mechanisms in the investigation of specific chemical changes.

For example, NMR, being very sensitive to changes in molecular motion, can be used to detect the spin–spin relaxation time of chains¹⁰ and to gain useful structural information about the network, such as the distinction of crosslinked chains from free and dangling chains. As is shown in Scheme 1, a crosslinked rubber includes three parts. The first is constituted by crosslinked chains with two ends connected to the network. The second is composed of dangling chains with free ends and loops. The third is free chains (unvulcanized molecules) and small-molecule additives. These three parts have different mobilities and exhibit different spin–spin relaxation times in NMR



Scheme 1. Different chain structures in a crosslinked rubber. [Color figure can be viewed in the online issue, which is available at wileyonlinelibrary.com.]

measurements. Crosslinked chains have the lowest mobility and, therefore, the shortest relaxation time because of the fixed ends. The longest relaxation time belongs to free molecules, which have the highest mobility with two free ends. Dangling chains and loops have moderate mobilities and moderate relaxation times. The parameter $(Qmrl)^{1/2}$ was used to represent the relative crosslinking degree, but it accounts only for the crosslinked part. Dangling chains and loops are not included in the calculation.

An indirect measure of the crosslinking density is the determination of the swelling ratio, a very common, simple, and low-cost method based on the ability of a good solvent to swell the network.¹¹ Solvent extraction is also a simple method for measuring the crosslinking degree via the extraction of soluble parts from the sample. Because the solvent can only extract free chains and additives, the dangling chains and loops remain in the insoluble part. Therefore, the gel content result includes the contributions of the crosslinked part, dangling chains, and loops. Both $(Qmrl)^{1/2}$ and the gel content account for the fraction of molecules in the crosslinking network, and they report the crosslinking degree (i.e., how many molecules are included in the network structure). However, $(Qmrl)^{1/2}$ only concerns the crosslinked part, whereas the gel content also includes dangling chains and loops that connect to the network. In contrast, the solvent swelling test reflects the average lattice size in the crosslinking network (the crosslinking density). The crosslinking degree and the crosslinking density are completely different concepts. They focus on different structural characteristics of a network and may change separately during thermal aging. However, in studies reported in the literature, they have often been mixed, and the network structure has not been investigated clearly.

In this study, we carried out the investigation of crosslinking (the changes of the crosslinking degree and the crosslinking density) during the thermooxidative aging of an NBR compound using NMR, swelling, and solvent extraction methods. Each experimental methodology provides different information on the rubber network topology and, in particular, the crosslinking density. The combination of these methods provides a

complete profile of the change of the network structure and allows us to obtain a good understanding of the network structural evolution, the rubber thermal aging behavior, and its relationship with the mechanical properties.

EXPERIMENTAL

Vulcanized NBR compound samples were supplied by SKF Sealing Solution. In addition to NBR, carbon black, a vulcanization package, silane, a plasticizer, and an antioxidant package were also included in the composition. Accelerated aging tests were carried out in temperature-controlled, air-circulating ovens at 60, 80, 100, and 125°C. Low-dimensional NMR (NM120, Shanghai Niumai Co., Ltd.) measurement was performed on the aged samples. The parameter $(Qmrl)^{1/2}$ was used to represent the relative crosslinking degree.¹⁰ Solvent extraction was carried out by the placement of the aged samples in refluxing xylene for 8 h to extract linear chains and small molecules. The samples were then placed in a vacuum chamber and heated to drive off any residue of the solvent. The gel content, which is the ratio of the insoluble mass to the initial mass, was used to show the crosslinking degree. The equilibrium swelling method was also performed by the immersion of the aged samples in methyl ethyl ketone for 96 h. The volume fraction of the polymer at swollen equilibrium (V2M) was used to characterize the crosslinking density as follows:

$$V2M = \frac{\frac{I \times F}{GP}}{\frac{I \times F}{GP} + \frac{S - D}{GS}}$$

where I is the initial weight, D is the dried weight, F is the weight fraction of the polymer in the compound, GP is the specific gravity of the polymer, S is the swollen weight, and GS is the specific gravity of the swelling solvent.

To observe the chemical changes on the sample surface during aging, attenuated total reflection (ATR)–Fourier transform infrared (FTIR) spectroscopy (Thermo-Nicolet 6700) was applied. The relative changes in the hydroxyl groups, carbonyl groups, and unsaturated species with respect to the $-\text{CN}$ bond (used as a reference because this band did not change obviously during the thermal aging), namely, $L_{\text{OH}}/L_{\text{CN}}$, $L_{\text{C=O}}/L_{\text{CN}}$, and $L_{\text{C=C}}/L_{\text{CN}}$, were used to detect chemical changes in NBR samples. The mechanical properties, including the hardness and Young's modulus, were also tested.⁹ Tensile tests were carried out on dumbbell-shape specimens at room temperature according to the standard ASTM D 412 with a Hounsfield H25KS testing machine. The tensile strength and elongation at break were the average values of three measurements. The surface hardness was measured with a Zwickdurometer (Shore A) according to the ASTM D 2240 standard test method.

RESULTS AND DISCUSSION

Figure 1 shows the crosslinking degree changes in NBR aged at 125°C as a function of time via NMR and solvent extraction, respectively. There was a rapid increase for both $(Qmrl)^{1/2}$ and the gel content during the first 48 h; this could be attributed to the loss of volatile additives, such as paraffin and antioxidants.⁹ With increasing aging time, the gel content increased continuously, whereas $(Qmrl)^{1/2}$ passed through a maximum. According

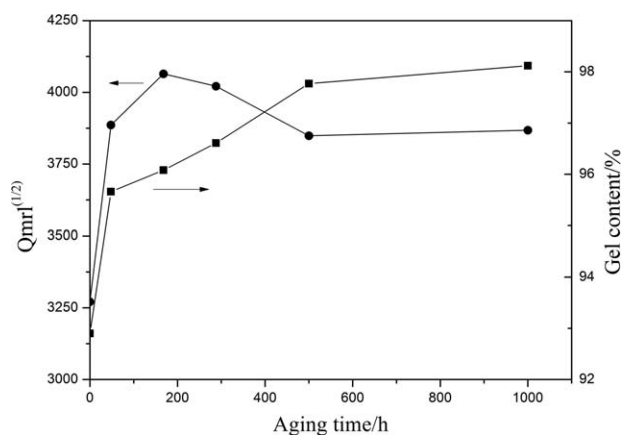


Figure 1. Changes in $Q_{mrl}^{1/2}$ and gel contents of NBR aged at 125°C as a function of the aging time.

to the previous discussion, it was reasonable to assume that during thermooxidative aging, more and more free chains were included in the network, so the gel content kept on increasing. However, a competition between further crosslinking and chain scissions during thermooxidative aging clearly took place. The

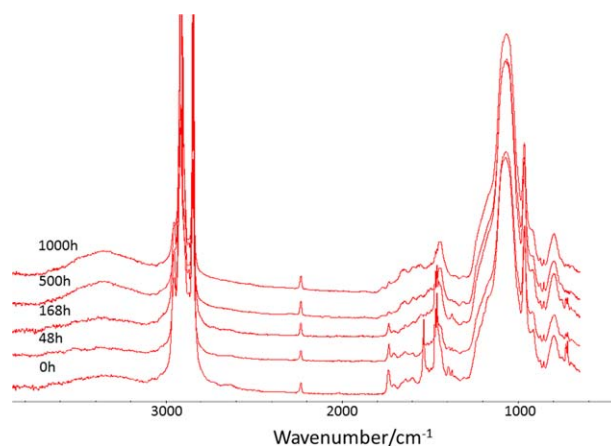


Figure 2. ATR-FTIR spectra of NBR with different aging times at 100°C. [Color figure can be viewed in the online issue, which is available at wileyonlinelibrary.com.]

amount of dangling chains began to increase after 168 h as the result of oxidation-induced chain scissions.^{9,12} Accordingly, the amount of fully crosslinked chains decreased from that time with the decrease in $(Q_{mrl})^{1/2}$. Because the dangling chains

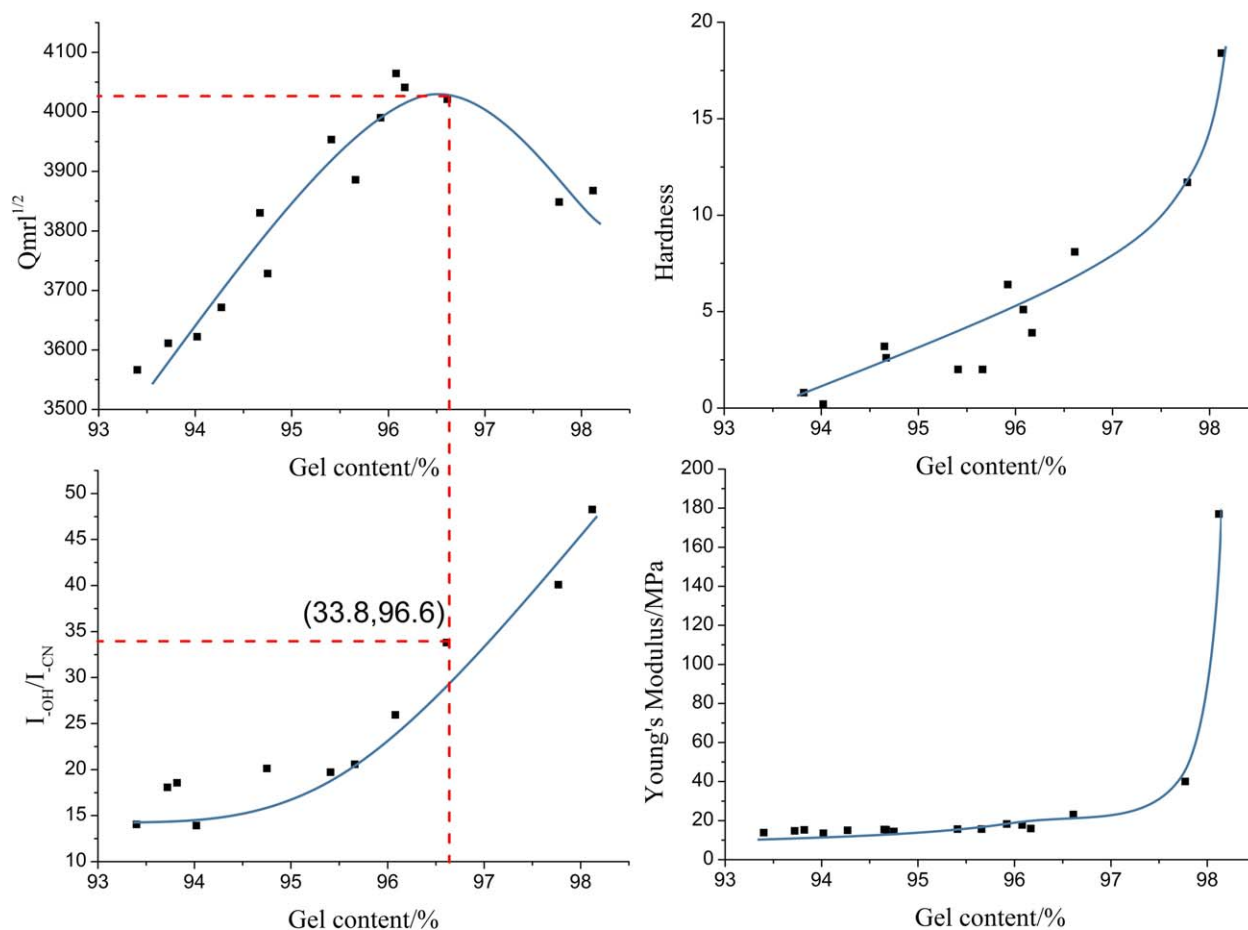


Figure 3. Changes in $Q_{mrl}^{1/2}$, L_{-OH}/L_{-CN} , hardness, and modulus with the gel content during aging. The master curves were made according to the time-temperature superposition principle with 100°C as the reference temperature. [Color figure can be viewed in the online issue, which is available at wileyonlinelibrary.com.]

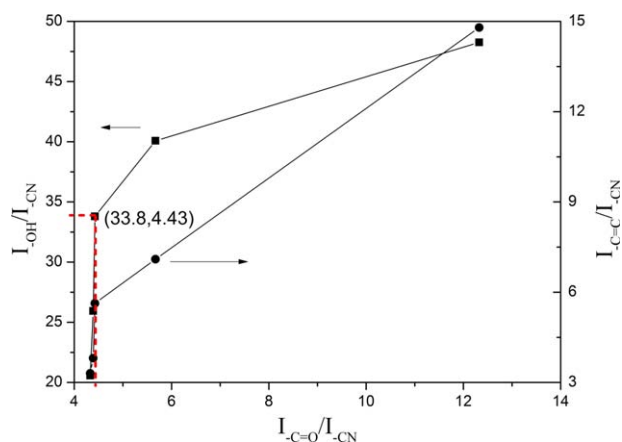


Figure 4. Relative changes in the chemical groups during aging. The master curves were made according to the time–temperature superposition principle with 100°C as the reference temperature. [Color figure can be viewed in the online issue, which is available at wileyonlinelibrary.com.]

were still in the network structure, their formation did not affect the gel content.

To gain better insight into the aging mechanism, chemical group changes were analyzed by means of ATR–FTIR spectroscopy. Figure 2 shows typical spectra with different aging times at 100°C. The peak at 3379 cm^{-1} belonged to hydroxyl groups ($-\text{OH}$). The peaks in the range 2800–3000 cm^{-1} were C–H vibrations. The peaks at 1735 and 1641 cm^{-1} were attributed to carbonyl groups ($-\text{C}=\text{O}$) and unsaturated species ($-\text{C}=\text{C}$), respectively. The peak at 2233 cm^{-1} belonged to the $-\text{CN}$ band. As was shown in our previous study,^{9,12} the time–temperature superposition principle was applied to build master curves, as shown in Figure 3, which here were proposed as a function of the gel content with the same shift factor. There was a transition point in the structural changes (with a gel content of 96.6%) to divide the two stages of aging. In the early stage, both $(Qmrl)^{1/2}$ and the hydroxyl groups increased with the gel content. In the later stage (gel content > 96.6%), $(Qmrl)^{1/2}$ began to decrease, whereas the content of hydroxyl groups increased at a higher rate. To illustrate the chemical changes

further, relative changes in the hydroxyl groups and unsaturated species with respect to carbonyl groups were plotted, as shown in Figure 4. The formation of hydroxyl groups represented the oxidation of the molecular chains. The formation of carbonyl groups occurred later; this was the result of further oxidation and chain scissions. The formation of unsaturated groups was, of course, the result of chain scissions. Before and after this transition point (gel content = 96.6%, $I_{\text{OH}}/I_{\text{CN}} = 33.8$), the relative ratios of the hydroxyl and unsaturated groups to carbonyl groups were different. In the early stage, hydroxyl and unsaturated groups increased much more quickly than carbonyl groups. In the late stage, the hydroxyl and unsaturated groups increased at slower rates compared with carbonyl groups, and unsaturated species showed a linear correlation with carbonyl groups. All these changes confirmed that chain scissions happened even at high gel content levels; this meant that further crosslinking and chain scissions happened simultaneously in the network.

It was worth noticing that in the later stage, although chain scissions took place, the crosslinking still continued, as evidenced by the increase in the gel content and especially V2M, as shown in Figure 5(a). The gel content slowed down after 500 h, whereas V2M kept increasing at a nearly constant rate. V2M was directly related to the crosslinking density. Its increase testified the decrease in the molecular weight between crosslinks. Therefore, the network structure became denser and denser until, at last (after 500 h), the mobility of the network chains was so low that the whole network became rigid. As a result, the hardness and the Young's modulus had a sudden upturn, as shown in Figure 3. It was also interesting to look at changes in the Young's modulus with the gel content and V2M, as proposed in Figure 5(b). Compared to the gel content, the Young's modulus was related more closely to V2M (the crosslinking density). That is, the Young's modulus depended more on the network density of NBR than on the molecular fraction in the network. More molecules in the network (higher crosslinking degree) did not certainly lead to a higher crosslinking density and, thus, a higher rigidity. Furthermore, the thermal oxidation of the network did not certainly lead to the mechanical

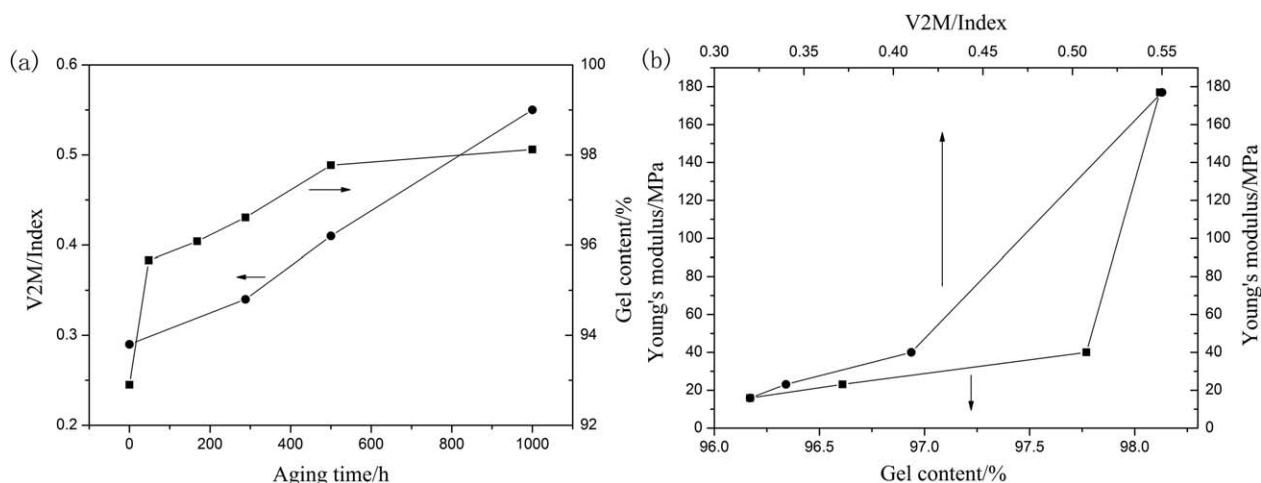
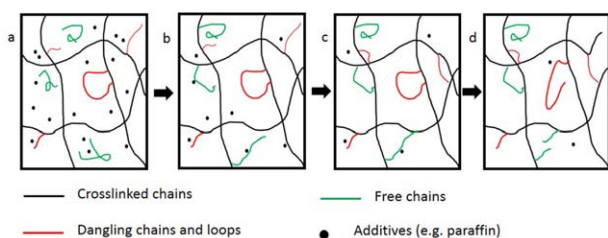


Figure 5. (a) Changes in V2M and gel contents at 125°C with the aging time. (b) Changes in the modulus with the gel content and V2M at 125°C.



Scheme 2. Changes in the NBR network structure during thermooxidation. [Color figure can be viewed in the online issue, which is available at wileyonlinelibrary.com.]

property changes unless it gave rise to significant changes in the crosslinking density of the network.

On the basis of the observations and measurements so far discussed, a hypothesis of the NBR network structural changes during thermooxidative aging is proposed in Scheme 2. In the beginning, free chains further crosslinked and joined the network; both the crosslinking degree and the crosslinking density increased. This proceeded until the majority of the free chains were crosslinked [Scheme 2(b)]. From then on, as nearly no new chains were introduced into the network, the crosslinking degree remained nearly constant, as measured by the gel content. Meanwhile, the crosslinking density (V2M) still increased with a decrease in the molecular weight between crosslinks [Scheme 2(c)]. The network became tighter and tighter until, at last, a rigid network formed, with an abrupt increase in the hardness and the Young's modulus.

The oxidation of NBR during aging gave rise to two results. First, oxidation induced extra crosslinking through the recombination of free radicals. Second, oxidation caused chain scissions in the network, especially at high temperatures. More carbonyl groups formed (shown in Figure 4), and dangling chains appeared [with the decrease in $(Qmrl)^{1/2}$; Figure 3]. Because it is nearly impossible for a crosslinked chain to break its two ends from the network at the same time, dangling chains other than free chains were generally formed as a result of the chain scissions [Scheme 2(d)]. That is why we only observed the decrease in $(Qmrl)^{1/2}$ but not one in the gel content.

CONCLUSIONS

In summary, in this article, we have mainly explained the different crosslinking trends of NBR during thermooxidative aging via the NMR, solvent extraction, and solvent swelling methods.

We have explicitly illustrated the distinction of these three methods when describing rubber network topology. The aging behavior of NBR could be interpreted on their basis. On one hand, the network became denser and harder because of the continuous increase in the crosslinking density. On the other hand, network chains broke down after high oxidation. The trends in crosslinking could be well correlated with the chemical structural changes via the FTIR method. Thus, the good understanding of crosslinking from various aspects could help us better deduce the aging status of the sample.

ACKNOWLEDGMENTS

The authors are grateful to Shanghai Niumai Co. for its support of the NMR testing.

REFERENCES

- Xu, C. H.; Chen, Y. K.; Huang, J.; Zeng, X. R.; Ding, J. P. *J. Appl. Polym. Sci.* **2012**, *124*, 2240.
- Lee, J. H.; Bae, J. W.; Kim, J. S.; Hwang, T. J.; Park, S. D.; Park, S. H.; Yeo, T. M.; Kim, W.; Jo, N. *J. Macromol. Res.* **2011**, *19*, 555.
- Mostafa, A.; Abouel-Kasem, A.; Bayoumi, M. R.; El-Sebaie, M. G. *Mater. Des.* **2009**, *30*, 791.
- Kwak, S. B.; Choi, N. S. *Int. J. Automot. Technol.* **2011**, *12*, 401.
- Radhakrishnan, C. K.; Alex, R.; Unnikrishnan, G. *Polym. Degrad. Stab.* **2006**, *91*, 902.
- Ha-Anh, T.; Vu-Khanh, T. *Polym. Test.* **2005**, *24*, 775.
- Delor-Jestin, F.; Barrois-Oudin, N.; Cardinet, C.; Lacoste, J.; Lemaire, J. *Polym. Degrad. Stab.* **2000**, *70*, 1.
- Colom, X.; Andreu-Mateu, F.; Canavate, F. J.; Mujal, R.; Carrillo, F. *J. Appl. Polym. Sci.* **2009**, *114*, 2011.
- Zhao, J. H.; Yang, R.; Iervolino, R.; Barbera, S. *Rubber Chem. Technol.* **2013**, *86*, 591.
- Kuhn, W.; Barth, P.; Hafner, S.; Simon, G.; Schneider, H. *Macromolecules* **1994**, *27*, 5773.
- Flory, P. J. *J. Chem. Phys.* **1950**, *18*, 108.
- Zhao, J. H.; Yang, R.; Iervolino, R.; Barbera, S. Presented at 9th International Symposium on Weatherability, Tokyo, Japan, March 2013.